

## A Novel Cobalt Organic-Inorganic Hybrid Magnetic Nanocatalyst for Convenient Four-Component Synthesis of 3,4-Dihydropyridones

Maryam Barazandehdoust<sup>a</sup>, Manouchehr Mamaghani<sup>a,b\*</sup>, Hassan Kefayati<sup>a</sup>

*a) Department of Chemistry, Rasht Branch, Islamic Azad University, Rasht, Iran*

*b) Department of Chemistry, Faculty of Sciences, University of Guilan, P.O. Box 41335-1914, Rasht, Iran*

Received 16 July 2022; received in revised form 9 October 2022; accepted 14 November 2022 (DOI: 10.30495/IJC.2022.1959315.1938)

### ABSTRACT

Densely functionalized 3,4-dihydropyridones were synthesized by a four-component reaction of Meldrum's acid, ethyl acetoacetate, ammonium acetate, and proper aromatic aldehydes in the presence of novel organic-inorganic cobalt incorporated magnetic nanocatalyst ( $\gamma\text{-Fe}_2\text{O}_3\text{@HAp/Co(II)}$ ) using ethanol as a green solvent at reflux condition. This new synthetic method provided the target compounds in a high yield (70-95%) and lower reaction time (20-75 min). The protocol benefits from the high purity of the products, environmentally friendly, milder reaction conditions, recyclability of the catalyst, and facile workup procedure. The structure of the synthesized novel nanocatalyst was confirmed by FT-IR, XRD, FSEM, TEM, EDS, and TGA analyses. The catalyst was used in eight cycles without any notable variation in catalytic activities.

**Keywords:** 3,4-Dihydropyridone, One-pot, Four-component, Meldrum's acid, Nanocatalyst,  $\gamma\text{-Fe}_2\text{O}_3\text{@HAp/Co(II)}$ .

### 1. Introduction

The main challenges in modern synthetic organic chemistry and medicinal chemistry is tailoring efficient and benign synthetic routes for the facile synthesis of organic compounds. In this respect, to prepare desired organic products, the objective is to provide protocols with easy workup procedures, high yield, lower reaction time, and least waste production. Therefore, to achieve these goals, multicomponent reactions (MCRs) due to high selectivity and simplicity [1, 2] and nanocatalysts have been employed extensively in recent years. A literature survey reveals that using multicomponent reactions in the presence of nanocatalysts accelerate and highly facilitate the production of heterocyclic compounds and are more adhered to the concepts of green chemistry. Devising novel synthetic procedures with high structural diversity for the synthesis of heterocyclic compounds with a broad range of therapeutic applications have always been required [3, 4].

On the other hand, 1,4-dihydropyridines (1,4-DHP) are well-known heterocyclic compounds used as  $\text{Ca}^{+2}$  channel blockers [5,6]. They are the main structural unit found in a diverse biologically active compound as a vasodilator [7], anti-atherosclerotic [8], anti-diabetic [9], and bio protector agents. In addition, the 2-pyridone motif structurally close to 1,4-dihydropyridines is present in various products having beneficial biological and medicinal activities [10-12]. Due to the valuable synthetic and biological properties of pyridone derivatives, several synthetic methods have been reported for the heterocyclic compounds having pyridone scaffold [13-15]. More recently, catalysts such as SBA-Pr-SO<sub>3</sub>H [16] and SiO<sub>2</sub>-Pr-SO<sub>3</sub>H [17] have also been used for the synthesis of pyridones. Some of the reported procedures are suffering from harsh reaction conditions, lower yield, and longer reaction times; therefore, introducing benign, facile, and straightforward protocols for the synthesis of heterocycles with pyridone skeleton is still required.

Considering our ongoing research in introducing facile methods for the synthesis of heterocyclic compounds of synthetic and medicinal importance [12, 18-22], we

\*Corresponding author:

E-mail address: m-chem41@guilan.ac.ir;  
mchem41@gmail.com (M. Mamaghani)

decided to present the novel cobalt organic-inorganic hybrid magnetic nanocatalyst ( $\gamma\text{-Fe}_2\text{O}_3\text{@HAp/Co(II)}$ ) and evaluate its efficiency in the synthesis of 2(1*H*)-pyridone derivatives.

## 2. Experimental

### 2.1. General

The chemicals used in present report were purchased from Merck and Fluka Company and used without further purification. Power X-ray diffraction (XRD) was performed on a (PW1730 Philips diffractometer) with Cu K $\alpha$  ( $\lambda = 1.54056 \text{ \AA}$ ) radiation. The thermal stability of the functionalized  $\gamma\text{-Fe}_2\text{O}_3\text{@HAp/Co(II)}$  was investigated by Thermogravimetric analysis (TGA), differential scanning calorimetry (DSC), and differential thermal analysis (DTA). The thermal gravimetric treatment of the specimen was scanned from 25 to 600 °C at the rate of 25 °C/min under Ar atmosphere by using TA–SDT Q600 instrument.  $^1\text{H}$  NMR and  $^{13}\text{C}$  NMR experiment were recorded on a Bruker Advance 300 MHz spectrometers.  $^1\text{H}$  NMR and  $^{13}\text{C}$  NMR spectra were referenced relative to peaks of the deuterated solvent or TMS. (FT-IR) spectra were taken on a Thermo (USA) FT-IR spectrophotometer. The cobalt contents of samples were measured by ICP-OES on a varian AGILENT Model 7900 inductively coupled plasma optical emission with axial injection. Scanning electron microscopy (FESEM) has been performed using a TESCAN Model MIRA3 XMU VP-FESEM microscope with a scanning range from 3 to 30 keV. Melting points were recorded on an electrothermal IA9100 apparatus in open capillary tubes. TEM micrograph images were obtained on a Philips CM120 microscope.

### 2.2. Synthesis of $\gamma\text{-Fe}_2\text{O}_3\text{@HAp/Co(II)}$

$[\gamma\text{-Fe}_2\text{O}_3\text{@HAp-Si-(CH}_2)_3\text{-NH}_2]_2$  were prepared via a simple method [23, 24].  $\text{Fe}_3\text{O}_4$  MNP was prepared according to the previous report [25] and was separated by an external magnet and washed with dry ethanol to give the catalyst precursor 3. A stirring blend of 3 (0.8 g) and  $\text{CoCl}_2$  (0.104 g) in ethanol (15 mL) was kept at room temperature for 12 h. The light brown precipitate was separated, washed frequently with ethanol, and dried under vacuum at room temperature to produce the target  $\gamma\text{-Fe}_2\text{O}_3\text{@HAp/Co(II)}$  (0.5 g).

### 2.3 General procedure for preparation of (5a-o)

To evaluate the application of the synthesized Co nanocatalyst in a typical preparation of 3,4-dihydropyridones, Meldrum's acid (1.0 mmol), ethyl

acetoacetate (1.0 mmol), aromatic aldehyde (1.0 mmol), ammonium acetate (3.0 mmol) and 10 mg, 0.22 mol% of supported  $\gamma\text{-Fe}_2\text{O}_3\text{@HAp/Co(II)}$  were added to 2 mL of ethanol, and the reaction mixture was stirred at 78 °C. The progress of the reaction was checked by TLC. After completion of the reaction, the catalyst was separated using an external magnet and washed several times with ethanol, and the resultant organic solution was evaporated under a vacuum to produce a crude product which was purified by chromatography to produce the target products. The separated catalyst was rinsed with hot EtOH and deionized water (three times) and was dried. The recovered catalyst was used again for carrying out the next reaction cycle.

### 2.4. Spectral data of the selected products:

**2.4.1 Ethyl 4-(4-bromophenyl)-2-methyl-6-oxo-1,4,5,6-tetrahydropyridine-3-carboxylate (5a).** Light-yellow solid, m.p. = 185-187 °C; FT-IR (KBr,  $\text{cm}^{-1}$ ): 3234 (NH), 1693, 1627 (C=O), 1197 (C-O-C), 1085 (C-Br)  $\text{cm}^{-1}$ .  $^1\text{H}$  NMR (300 MHz,  $\text{CDCl}_3$ ):  $\delta_{\text{H}} = 7.98$  (s, 1H), 7.43 (d,  $J = 8.4$  Hz, 2H), 7.09 (d,  $J = 8.4$  Hz, 2H), 4.24 (d,  $J = 7.5$  Hz, 1H), 4.09-4.20 (m, 2H), 2.95 (dd,  $J = 16.5, 8.1$  Hz, 1H), 2.68 (dd,  $J = 16.5, 1.2$  Hz, 1H), 2.43 (s, 3H), 1.22 (t,  $J = 7.05$  Hz, 3H).  $^{13}\text{C}$  NMR (75 MHz,  $\text{CDCl}_3$ ):  $\delta_{\text{C}} = 170.4, 166.6, 146.2, 141.2, 131.9, 128.5, 120.8, 107.0, 60.4, 37.9, 37.5, 19.2, 14.2$  ppm. Anal. Calc. for  $\text{C}_{15}\text{H}_{16}\text{BrNO}_3$  (338.20): C, 53.27; H, 4.77; N, 4.14; Found: C, 53.15; H, 4.64; N, 4.01.

**2.4.2 Ethyl 4-(2,4-dichlorophenyl)-2-methyl-6-oxo-1,4,5,6-tetrahydropyridine-3-carboxylate (5f).** Light-yellow solid, m.p. = 180-183 °C; FT-IR (KBr,  $\text{cm}^{-1}$ ): 3214 (NH), 1697, 1636 (C=O) 1289, 1204 (C-O-C), 1100 (C-Cl)  $\text{cm}^{-1}$ .  $^1\text{H}$  NMR (300 MHz,  $\text{CDCl}_3$ ):  $\delta_{\text{H}} = 8.16$  (s, 1H), 7.44 (d,  $J = 2.1$  Hz, 1H), 7.17 (dd,  $J = 8.4, 2.1$  Hz, 1H), 7.00 (d,  $J = 8.4$  Hz, 1H), 4.70 (d,  $J = 7.8$  Hz, 1H), 4.02- 4.15 (m, 2H), 2.94 (dd,  $J = 16.8, 8.4$  Hz, 1H), 2.68 (dd,  $J = 16.8, 0.9$  Hz, 1H), 2.50 (s, 3H), 1.16 (t,  $J = 7.20$  Hz, 3H).  $^{13}\text{C}$  NMR (75 MHz,  $\text{CDCl}_3$ ):  $\delta_{\text{C}} = 170.1, 166.3, 147.4, 137.3, 133.9, 133.4, 129.9, 128.2, 127.4, 105.9, 60.3, 36.2, 34.7, 19.0, 14.0$  ppm. Anal. Calc. for  $\text{C}_{15}\text{H}_{15}\text{Cl}_2\text{NO}_3$  (328.19): C, 54.90; H, 4.61; N, 4.27; Found: C, 54.78; H, 4.45; N, 4.12.

**2.4.3 Ethyl 4-(2-bromophenyl)-2-methyl-6-oxo-1,4,5,6-tetrahydropyridine-3-carboxylate (5g).** Light-yellow solid, m.p. = 189-192 °C; FT-IR (KBr,  $\text{cm}^{-1}$ ): 3224 (NH), 1695, 1629 (C=O), 1283, 1203 (C-O-C), 1087 (C-Br)  $\text{cm}^{-1}$ .  $^1\text{H}$  NMR (300 MHz,  $\text{CDCl}_3$ ):  $\delta_{\text{H}} = 8.55$  (s, 1H), 7.61 (dd,  $J = 8.1, 0.9$  Hz, 1H), 7.23 (t,  $J = 6.9$  Hz, 1H), 7.06-7.13 (m, 2H), 4.73 (d,  $J = 8.1$  Hz, 1H), 3.98-4.15 (m, 2H), 2.94 (dd,  $J = 16.8, 8.4$  Hz, 1H), 2.72

(dd,  $J = 16.8, 1.8$  Hz, 1H), 2.48 (s, 3H), 1.14 (t,  $J = 7.05$  Hz, 3H).  $^{13}\text{C}$  NMR (75 MHz,  $\text{CDCl}_3$ ):  $\delta_c = 170.7, 166.5, 147.3, 140.3, 133.4, 128.6, 127.8, 127.3, 123.9, 106.4, 60.2, 37.7, 36.5, 18.8, 14.0$  ppm. Anal. Calc. for  $\text{C}_{15}\text{H}_{16}\text{BrNO}_3$  (338.20): C, 53.27; H, 4.77; N, 4.14; Found: C, 53.12; H, 4.59; N, 4.05.

#### 2.4.4 Ethyl 4-(3-methoxyphenyl)-2-methyl-6-oxo-1,4,5,6-tetrahydropyridine-3-carboxylate (5i).

Light-yellow solid, m.p. = 161-164 °C; FT-IR (KBr,  $\text{cm}^{-1}$ ): 3221 (NH), 1696, 1628 (C=O), 1279, 1196, 1090 (CO)  $\text{cm}^{-1}$ .  $^1\text{H}$  NMR (300 MHz,  $\text{CDCl}_3$ ):  $\delta_H = 7.90$  (s, 1H), 7.20-7.25 (m, 1H), 6.76-6.82 (m, 3H), 4.26 (d,  $J = 7.2$  Hz, 1H), 4.09-4.20 (m, 2H), 3.80 (s, 3H, MeO), 2.95 (dd,  $J = 16.5, 8.1$  Hz, 1H), 2.73 (dd,  $J = 16.5, 1.2$  Hz, 1H), 2.43 (s, 3H), 1.22 (t,  $J = 7.05$  Hz, 3H).  $^{13}\text{C}$  NMR (75 MHz,  $\text{CDCl}_3$ ):  $\delta_c = 170.6, 166.8, 159.8, 145.9, 143.8, 129.8, 119.0, 113.0, 111.7, 107.3, 60.2, 55.2, 38.0, 37.9, 19.2, 12.2$  ppm. Anal. Calc. for  $\text{C}_{16}\text{H}_{19}\text{NO}_4$  (289.33): C, 66.42; H, 6.62; N, 4.84; Found: C, 66.34; H, 6.47; N, 4.71.

#### 2.4.5 Ethyl 4-(2-methoxyphenyl)-2-methyl-6-oxo-1,4,5,6-tetrahydropyridine-3-carboxylate (5j).

Light-yellow solid, m.p. = 185-187 °C; FT-IR (KBr,  $\text{cm}^{-1}$ ): 3232 (NH), 1695, 1632 (C=O), 1287, 1198, 1083 (C-O)  $\text{cm}^{-1}$ .  $^1\text{H}$  NMR (300 MHz,  $\text{CDCl}_3$ ):  $\delta_H = 7.53$  (s, 1H), 7.3 (dt,  $J = 8.1, 1.2$  Hz, 1H), 7.01 (d,  $J = 6.6$  Hz, 1H), 6.83-6.90 (m, 2H), 4.62 (d,  $J = 7.8$  Hz, 1H), 4.05-4.18 (m, 2H), 3.87 (s, 3H), 2.87 (dd,  $J = 16.5, 8.1$  Hz, 1H), 2.74 (dd,  $J = 16.5, 1.8$  Hz, 1H), 2.46 (s, 3H), 1.17 (t,  $J = 7.2$  Hz, 3H).  $^{13}\text{C}$  NMR (75 MHz,  $\text{CDCl}_3$ ):  $\delta_c = 170.8, 167.0, 159.8, 146.1, 129.1, 128.1, 127.1, 120.4, 110.7, 106.4, 60.1, 55.2, 36.4, 32.6, 19.2, 14.1$  ppm. Anal. Calc. for  $\text{C}_{16}\text{H}_{19}\text{NO}_4$  (289.33): C, 66.42; H, 6.62; N, 4.84; Found: C, 66.32; H, 6.45; N, 4.73.

#### 2.4.6 Ethyl 2-methyl-6-oxo-4-(p-tolyl)-1,4,5,6-tetrahydropyridine-3-carboxylate (5k).

Light-yellow solid, m.p. = 182-184 °C; FT-IR (KBr,  $\text{cm}^{-1}$ ): 3234 (NH), 1692, 1628 (C=O), 1288, 1197 (C-O-C)  $\text{cm}^{-1}$ .  $^1\text{H}$  NMR (300 MHz,  $\text{CDCl}_3$ ):  $\delta_H = 7.29$  (s, 1H), 7.10 (s, 4H), 4.26 (d,  $J = 6.9$  Hz, 1H), 4.09-4.20 (m, 2H), 2.94 (dd,  $J = 16.5, 7.8$  Hz, 1H), 2.72 (dd,  $J = 16.5, 1.5$  Hz, 1H), 2.42 (s, 3H), 2.33 (s, 3H), 1.23 (t,  $J = 7.05$  Hz, 3H).  $^{13}\text{C}$  NMR (75 MHz,  $\text{CDCl}_3$ ):  $\delta_c = 170.3, 166.9, 145.3, 139.1, 136.5, 129.4, 126.6, 107.7, 60.2, 38.0, 37.5, 21.0, 19.4, 14.2$  ppm. Anal. Calc. for  $\text{C}_{16}\text{H}_{19}\text{NO}_3$  (273.33): C, 70.31; H, 7.01; N, 5.12; Found: C, 70.18; H, 7.13; N, 5.02.

#### 2.4.6 Ethyl 4-(2,6-dichlorophenyl)-2-methyl-6-oxo-1,4,5,6-tetrahydropyridine-3-carboxylate (5l).

Light-yellow solid, m.p. = 233-235 °C; FT-IR (KBr,  $\text{cm}^{-1}$ ): 3225 (NH), 1692, 1629 (C=O), 1290, 1219 (C-O-C), 1094 (C-Cl)  $\text{cm}^{-1}$ .  $^1\text{H}$  NMR (300 MHz,  $\text{CDCl}_3$ ):  $\delta_H = 7.54$  (s, 1H), 7.32 (d,  $J = 9.0$  Hz, 2H), 7.12 (t,  $J = 7.5$  Hz, 1H), 5.12- 5.19 (m, 1H), 3.88-4.01 (m, 2H), 2.95 (dd,  $J = 18.0, 9.0$  Hz, 1H), 2.84 (dd,  $J = 18.0, 9.0$  Hz, 1H), 2.34 (s, 3H), 0.93 (t,  $J = 7.5$  Hz, 3H).  $^{13}\text{C}$  NMR (75 MHz,  $\text{CDCl}_3$ ):  $\delta_c = 169.4, 166.5, 143.2, 138.9, 135.0, 129.2, 128.1, 105.7, 59.9, 36.2, 33.7, 19.1, 13.6$  ppm. Anal. Calc. for  $\text{C}_{15}\text{H}_{15}\text{Cl}_2\text{NO}_3$  (328.19): C, 54.90; H, 4.61; N, 4.27; Found: C, 54.76; H, 4.72; N, 4.39.

#### 2.4.7 Ethyl 4-(4-hydroxy-3-methoxyphenyl)-2-methyl-6-oxo-1,4,5,6-tetrahydropyridine-3-carboxylate (5m).

Light-yellow solid, m.p. = 291-294 °C; FT-IR (KBr,  $\text{cm}^{-1}$ ): 3698, 3396 (O-H), 3220 (NH), 1673, 1633 (C=O), 1289, 1260, 1222, 1092 (C-O)  $\text{cm}^{-1}$ .  $^1\text{H}$  NMR (300 MHz,  $\text{CDCl}_3$ ):  $\delta_H = 7.21$  (s, 1H), 6.83 (d,  $J = 8.1$  Hz, 1H), 6.68-6.74 (m, 2H), 5.54 (s, 1H), 4.13-4.27 (m, 3H), 3.88 (s, 3H), 2.93 (dd,  $J = 16.5, 7.8$  Hz, 1H), 2.73 (dd,  $J = 16.5, 1.5$  Hz, 1H), 2.42 (s, 3H), 1.25 (t,  $J = 7.05$  Hz, 3H).  $^{13}\text{C}$  NMR (75 MHz,  $\text{CDCl}_3$ ):  $\delta_c = 170.2, 166.9, 146.6, 145.1, 144.6, 134.0, 119.2, 114.4, 109.5, 107.9, 60.3, 55.8, 38.2, 37.6, 14.2$  ppm. Anal. Calc. for  $\text{C}_{16}\text{H}_{19}\text{NO}_5$  (305.33): C, 62.94; H, 6.27; N, 4.59; Found: C, 62.83; H, 6.16; N, 4.42.

#### 2.4.8 Ethyl 2-methyl-6-oxo-4-(m-tolyl)-1,4,5,6-tetrahydropyridine-3-carboxylate (5n).

Light-yellow solid, m.p. = 131-133 °C; FT-IR (KBr,  $\text{cm}^{-1}$ ): 3219 (NH), 1695, 1630 (C=O), 1282, 1200, 1081 (C-O)  $\text{cm}^{-1}$ .  $^1\text{H}$  NMR (300 MHz,  $\text{CDCl}_3$ ):  $\delta_H = 7.49$  (s, 1H), 7.18 (t,  $J = 7.8$  Hz, 1H), 6.99-7.06 (m, 3H), 4.25 (d,  $J = 7.5$  Hz, 1H), 4.10-4.20 (m, 2H), 2.95 (dd,  $J = 16.5, 8.1$  Hz, 1H), 2.73 (dd,  $J = 16.5, 1.5$  Hz, 1H), 2.43 (s, 3H), 2.34 (s, 3H), 1.23 (t,  $J = 7.05$  Hz, 3H).  $^{13}\text{C}$  NMR (75 MHz,  $\text{CDCl}_3$ ):  $\delta_c = 170.3, 166.9, 145.4, 142.1, 138.3, 128.6, 127.7, 127.5, 123.6, 107.6, 60.2, 38.0, 37.9, 21.5, 19.3, 14.2$  ppm. Anal. Calc. for  $\text{C}_{16}\text{H}_{19}\text{NO}_3$  (273.33): C, 70.31; H, 7.01; N, 5.12; Found: C, 70.19; H, 6.92; N, 4.96.

#### 2.4.9 Ethyl 4-(3-chlorophenyl)-2-methyl-6-oxo-1,4,5,6-tetrahydropyridine-3-carboxylate (5o).

Light-yellow solid, m.p. = 177-180 °C; FT-IR (KBr,  $\text{cm}^{-1}$ ): 3225 (NH), 1695, 1630 (C=O), 1284, 1205 (C-O-C), 1087 (C-Cl)  $\text{cm}^{-1}$ .  $^1\text{H}$  NMR (300 MHz,  $\text{CDCl}_3$ ):  $\delta_H = 7.54$  (s, 1H), 7.40-7.43 (m, 1H), 7.17-7.20 (m, 2H), 7.06-7.09 (m, 1H), 4.77 (d,  $J = 7.5$  Hz, 1H), 3.99-4.16 (m, 2H), 2.95 (dd,  $J = 16.6, 8.5$  Hz, 1H), 2.73 (dd,  $J = 16.6, 1.3$  Hz, 1H), 2.50 (s, 3H), 1.14 (t,  $J = 7.05$  Hz, 3H).  $^{13}\text{C}$  NMR (75 MHz,  $\text{CDCl}_3$ ):  $\delta_c = 169.8, 166.4, 146.9, 138.7, 133.2, 130.1, 128.3, 127.2, 127.1, 106.3, 60.2, 36.4, 35.1, 19.0, 14.0$  ppm. Anal. Calc. for  $\text{C}_{15}\text{H}_{16}\text{ClNO}_3$

(293.75): C, 61.33; H, 5.49; N, 4.77; Found: C, 61.21; H, 5.34; N, 4.89.

### 3. Results and Discussion

#### 3.1 Preparation of $\gamma\text{-Fe}_2\text{O}_3\text{@HAp/Co(II)}$

$\gamma\text{-Fe}_2\text{O}_3\text{@HAp}$  nanoparticles were synthesized by the conventional co-precipitation method with some modifications [23, 25-29]. Initially,  $\text{Fe}_3\text{O}_4$  nanoparticles were synthesized by using  $\text{FeCl}_2\cdot 4\text{H}_2\text{O}$  and  $\text{FeCl}_3\cdot 6\text{H}_2\text{O}$  as starting materials and ammonia as a precipitating agent. According to our previous report [26], a layer of hydroxyapatite (HAp) was coated on the surface of the  $\text{Fe}_3\text{O}_4$  nanoparticles and was calcinated at  $400\text{ }^\circ\text{C}$  to finish  $\gamma\text{-Fe}_2\text{O}_3\text{@HAp}$ . So obtained solid product was functionalized by 3-aminopropyltrimethoxysilane to finish an organic-inorganic hybrid. The prepared hybrid was reacted with 2-hydroxybenzaldehyde to give the desired magnetic nanocatalyst with a bi-dentate ligand. Finally, surface-bound ligands were complexed with cobalt (II) by using  $\text{CoCl}_2$  to furnish  $\gamma\text{-Fe}_2\text{O}_3\text{@HAp/Co(II)}$  (**Scheme 1**).

#### 3.2 Characterization of $\gamma\text{-Fe}_2\text{O}_3\text{@HAp/Co(II)}$

##### 3.2.1 XRD

In XRD of  $\gamma\text{-Fe}_2\text{O}_3\text{@HAp/Co(II)}$  (**Fig. 1a**), the diffraction peaks appeared at  $2\theta = 18.3^\circ, 26.1^\circ, 30.5^\circ, 32.4^\circ, 35.9^\circ, 39.9^\circ, 43.6^\circ, 47.0^\circ, 50.0^\circ, 53.6^\circ, 57.6^\circ, 63.3^\circ,$  and  $75.2^\circ$  are pertaining to the planes of (111), (211), (220), (112), (311), (310), (400), (222), (123), (004), (133), (150) and (602) respectively (**Fig. 1**) and

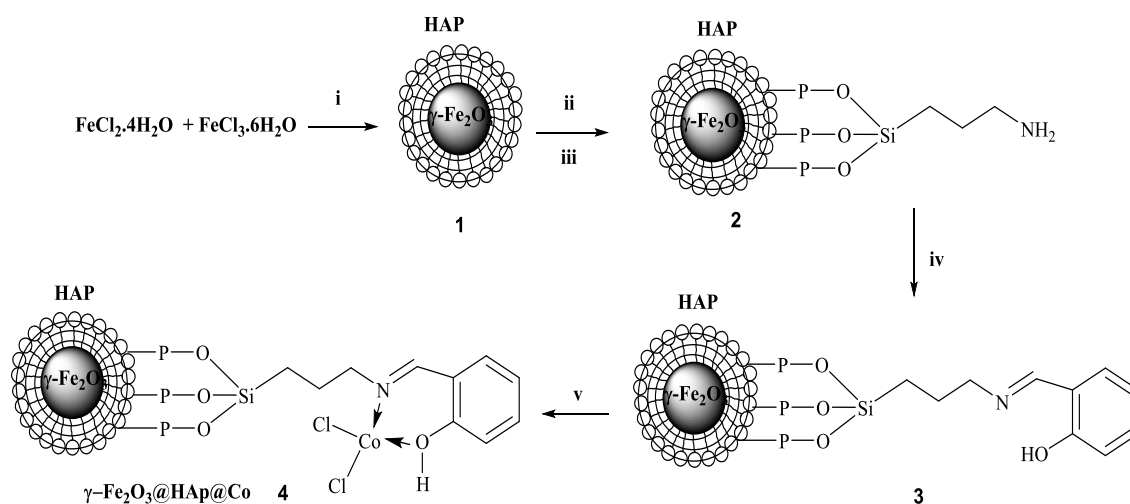
can be ascribed to  $\gamma\text{-Fe}_2\text{O}_3$  (JCPDS no 00-004-0755) and hydroxyapatite (JCPDS no 01-084-1998). The mean  $\gamma\text{-Fe}_2\text{O}_3\text{@HAp/Co(II)}$  size was estimated from the most severe peak (112) using Scherrer's equation [30] to be around 6.15 nm.

$$D_c = \frac{K \lambda}{\beta_{1/2} \cos \theta}$$

Where  $D_c$  is the crystallite diameter,  $K$  is the Scherrer constant (0.89),  $\lambda$  is the X-ray wavelength (0.1540 nm), and  $\beta_{1/2}$  is the full width at half maximum of the diffraction peak, and  $\theta$  is the diffraction angle of the peak.

##### 3.2.2. FT-IR

FT-IR spectrum of the prepared nanocatalyst is shown in **Fig. 2b** (in KBr). The absorption peak at  $458\text{ cm}^{-1}$  can be assigned to the Fe-O absorption in the maghemite [31]. The O-P-O surface phosphate groups in the hydroxyapatite shell emerged at  $566$  and  $602\text{ cm}^{-1}$  which were in overlap with Fe-O stretching. The P-O stretching emerged at  $1037\text{ cm}^{-1}$ . The bands at around  $1415$  and  $1447\text{ cm}^{-1}$  are associated to the aromatic C=C stretching; also, a band at  $1632\text{ cm}^{-1}$  produced by the C=N double bond verify that the organic linker is exactly immobilized onto the surface. Note that the C=N band is shifted to a higher wave number compared to the C=N stretching frequency of the catalyst precursor  $\gamma\text{-Fe}_2\text{O}_3\text{@HAp}$  (**Fig. 2a**) ( $1628\text{ cm}^{-1}$  rather than  $1632\text{ cm}^{-1}$ ). It implies that C=N and OH groups are coordinated to cobalt (Co) through the lone pair of N and O (**Fig. 2**).



Scheme 1. (i)  $\text{Ca}(\text{NO}_3)_2$ ,  $(\text{NH}_4)_2\text{HPO}_4$ ,  $\text{NH}_4\text{OH}$ , (ii) calcination, (iii) 3-aminopropyltrimethoxysilane, toluene, reflux, 48 h, (iv) 2-hydroxy benzaldehyde, dry EtOH, reflux, 24 h, (v)  $\text{CoCl}_2$ , EtOH, r.t., 12 h.

#### Scheme 1. Synthesis of $\gamma\text{-Fe}_2\text{O}_3\text{@HAp/Co(II)}$

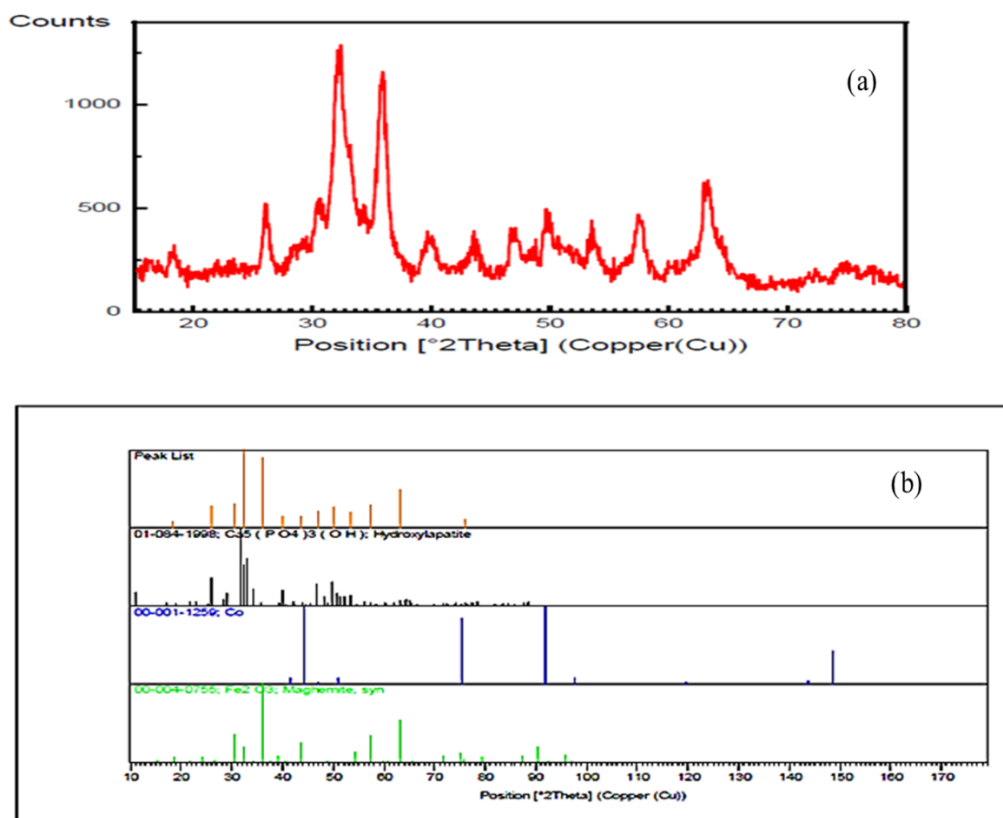


**Fig.1.** (a) XRD patterns of the  $\gamma\text{-Fe}_2\text{O}_3@HAp/Co(II)$ . (b) Identification of the X-ray diffraction phase of  $\gamma\text{-Fe}_2\text{O}_3@HAp/Co(II)$

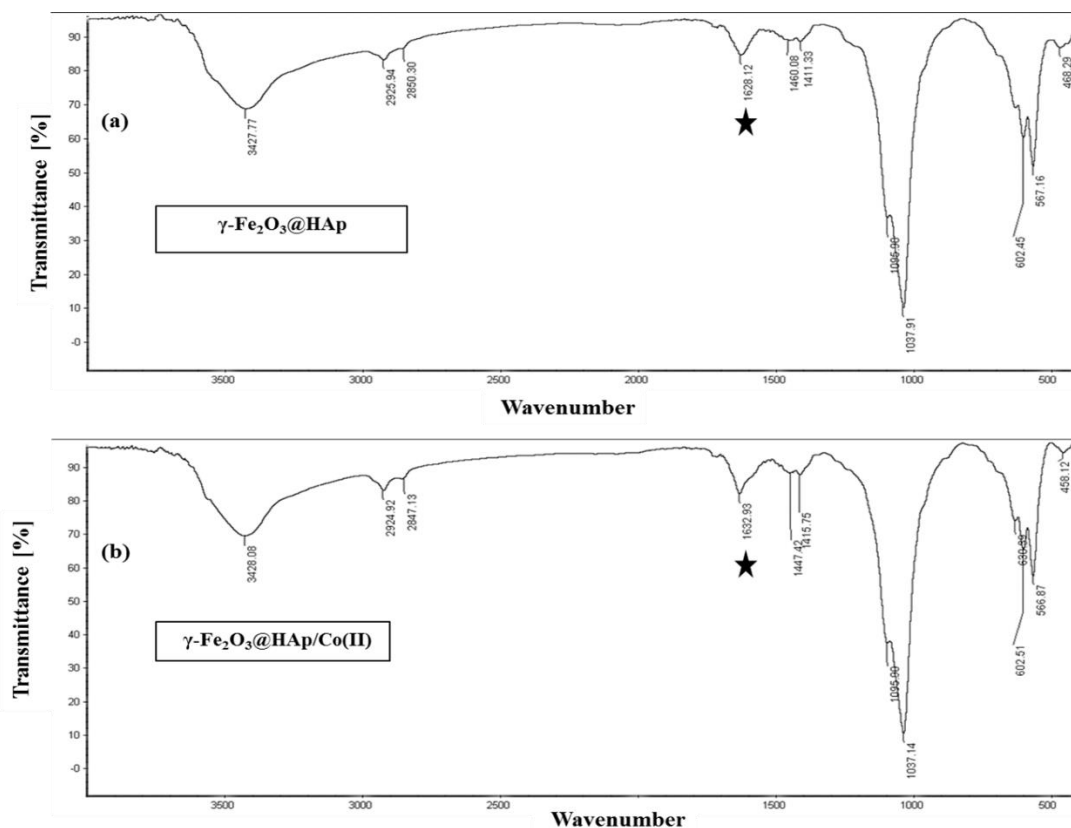


**Fig.2.** FT-IR spectrum of the catalyst (a)  $\gamma\text{-Fe}_2\text{O}_3@HAp$  and (b)  $\gamma\text{-Fe}_2\text{O}_3@HAp/Co(II)$ .

### 3.2.3 SEM

The SEM image (**Fig. 3**) of the  $\gamma\text{-Fe}_2\text{O}_3\text{@HAp/Co(II)}$  provides the average size of  $\gamma\text{-Fe}_2\text{O}_3\text{@HAp/Co(II)}$  to be around 17 nm (**Fig. 3** (a, b)). Also, the SEM image of the catalyst indicates the retention of the catalytic activity after recycling without any changes in morphology and size (after eight consecutive runs) (**Fig. 3c**).

### 3.2.4 VSM

A magnetic attribute of the  $\gamma\text{-Fe}_2\text{O}_3\text{@HAp/Co(II)}$  was done by the field sweeping from -20 to 20 KOe (-15000 to 15000 Oe). The M(H) hysteresis loop for the sample was with saturation magnetization ( $M_s$ ) value of  $16.07 \text{ emu g}^{-1}$  (**Fig. 4**).

### 3.2.5 EDS

The presence of Ca, P, Fe, Si, Co, and Cl, related to the nanocatalyst structure, are seen in the spectrum (**Fig. 5**). The proportion of cobalt: chlorine: nitrogen in the spectrum is calculated to be 1: 1.41: 3.56, respectively. The amount of cobalt in the synthesized  $\gamma\text{-Fe}_2\text{O}_3\text{@HAp/Co(II)}$  is 1.29% according to the EDS analysis, which is equivalent to  $\sim 0.22 \text{ mmol}$  cobalt per gram of  $\gamma\text{-Fe}_2\text{O}_3\text{@HAp/Co(II)}$ .

### 3.2.6 TGA

Thermal stability of  $\gamma\text{-Fe}_2\text{O}_3\text{@HAp/Co(II)}$  was performed at the range 25 to  $600^\circ\text{C}$  thermogravimetric analysis (TGA) (**Fig. 6**), which revealed weight loss of 12.40% that could be likely pertaining to the

evaporation of the external water and parsing of organic groups on the surface of  $\gamma\text{-Fe}_2\text{O}_3\text{@HAp/Co(II)}$ .

### 3.2.7 TEM

The TEM image of the  $\gamma\text{-Fe}_2\text{O}_3\text{@HAp/Co(II)}$  was also recorded (**Fig. 7a, b**). As can be seen from the histogram, the particle size ranges from 2.7 to 10 nanometers (**Fig. 7c, d**), but most particles have a size of 5 nanometers, which is accurately reported by the device to be 4.67 nanometers, that is consistent with the XRD result.

### 3.2.8 Catalytic activity of $\gamma\text{-Fe}_2\text{O}_3\text{@HAp/Co(II)}$ for the synthesis of 3,4-dihydropyridones

The catalytic activity of magnetic nanoparticles was evaluated in the multicomponent synthesis of 3,4-dihydropyridones derivatives (**Scheme 2**).

Initially, a reaction between Meldrum's acid (1.0 mmol), ethyl acetoacetate (1.0 mmol), 4-bromobenzaldehyde (1.0 mmol), ammonium acetate (3.0 mmol), in the presence of catalyst  $\gamma\text{-Fe}_2\text{O}_3\text{@HAp/Co(II)}$  was selected for optimization of the reaction conditions. In order to verify the solvent effect, different solvents were investigated, and the results are collected in **Table 1**. According to the results, ethanol is the most suitable solvent for this reaction. In the next step, the temperature effect on the yield and reaction time of model compound **5a** in ethanol was also studied (Entries 6-10) (**Table 1**).

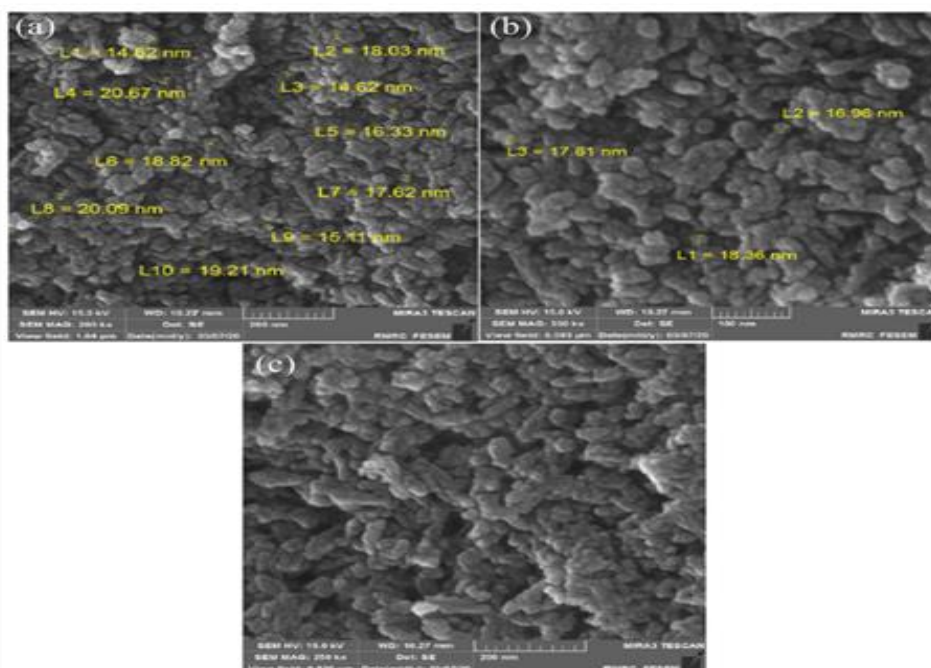


**Fig.3.** SEM image of the  $\gamma\text{-Fe}_2\text{O}_3\text{@HAp/Co(II)}$  (a, b) (nanoparticles with average size of 17 nm), (c) SEM image (after the tenth cycle) of the  $\gamma\text{-Fe}_2\text{O}_3\text{@HAp/Co(II)}$ .

The best result was obtained in ethanol at 78 °C. A comparison between a present catalyst and various acidic and the basic catalyst was also carried out, and the results revealed that the present catalyst ( $\gamma$ -Fe<sub>2</sub>O<sub>3</sub>@HAp/Co(II)) gives better efficiency in comparison with other catalysts. In addition, the effect of amount of  $\gamma$ -Fe<sub>2</sub>O<sub>3</sub>@HAp/Co(II) on the yield of model reaction was assessed. The best yield was achieved using 10 mg (0.22 mol%) nanocatalyst per 1 mmol substrate in ethanol under reflux conditions

(**Table 2**). Using the optimized reaction conditions, versatile derivatives of 3,4-dihydropyridones were synthesized in high to excellent yields and lower reaction times (**Table 3**). In this protocol, the catalyst was conveniently separated by an external magnet, washed with hot ethanol, deionized water, dried, and used in the next run. A comparison of present method for the synthesis of 3,4-dihydropyridones with various reported ones was also done (**Table 4**)

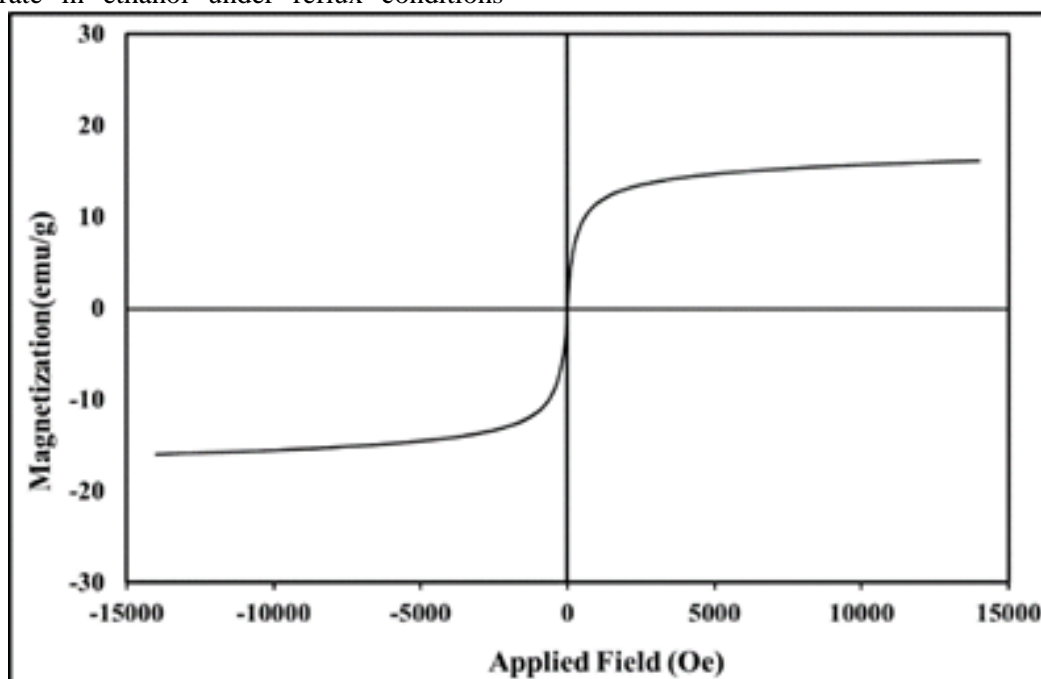


Fig.4. VSM curve of  $\gamma$ -Fe<sub>2</sub>O<sub>3</sub>@HAp/Co(II)

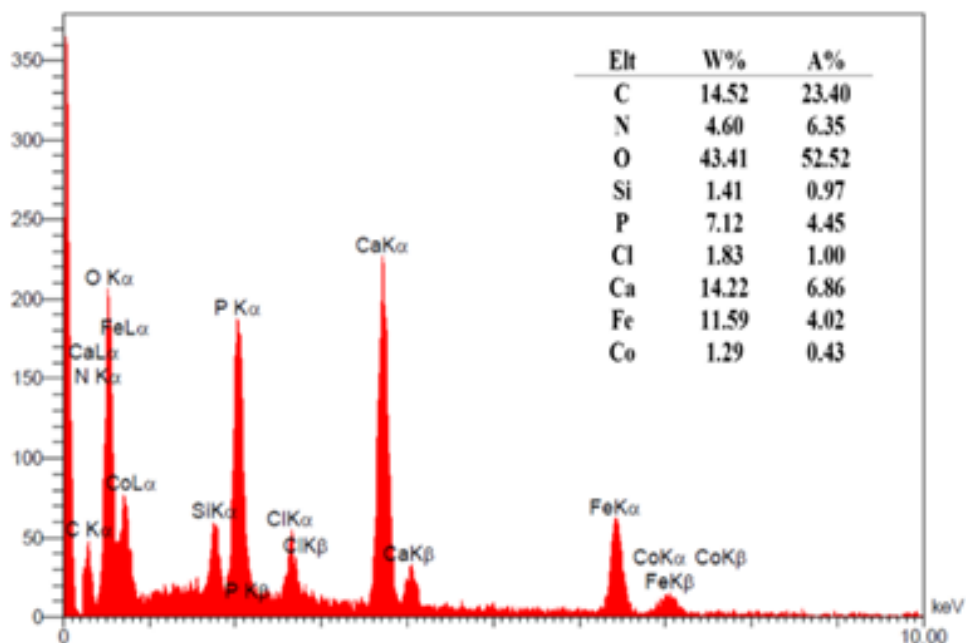


Fig.5. EDS spectra of  $\gamma$ -Fe<sub>2</sub>O<sub>3</sub>@HAp/Co(II)

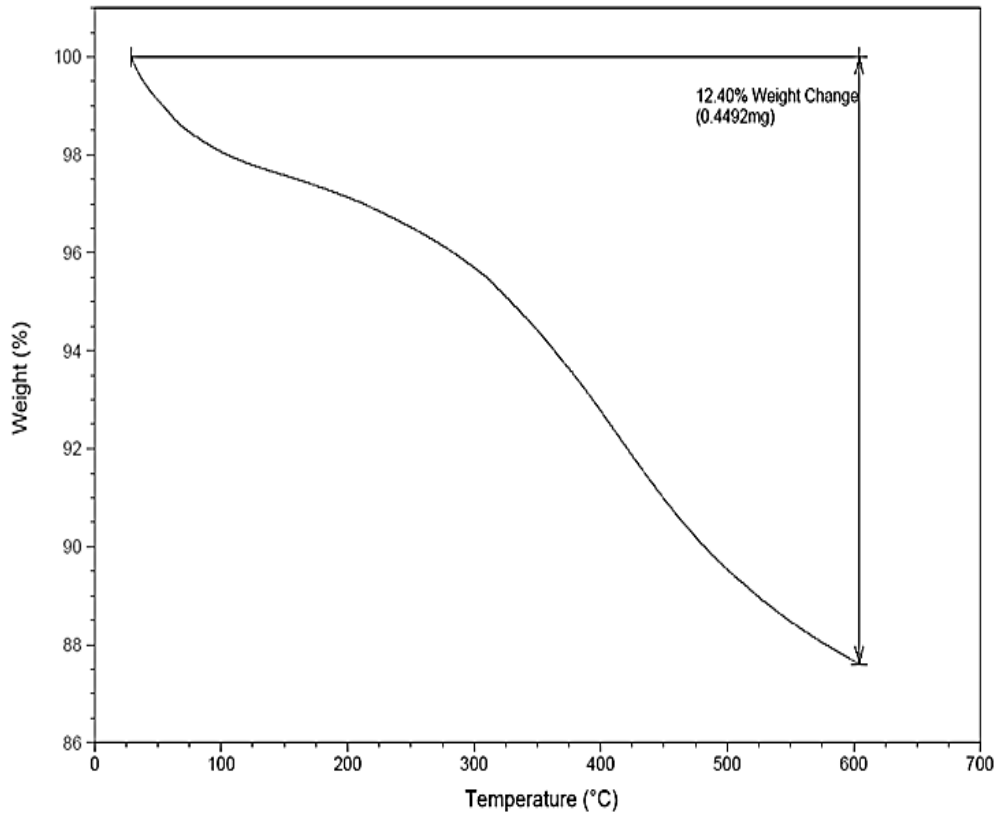


Fig.6. Total Thermogram of the  $\gamma\text{-Fe}_2\text{O}_3\text{@HAp/Co(II)}$

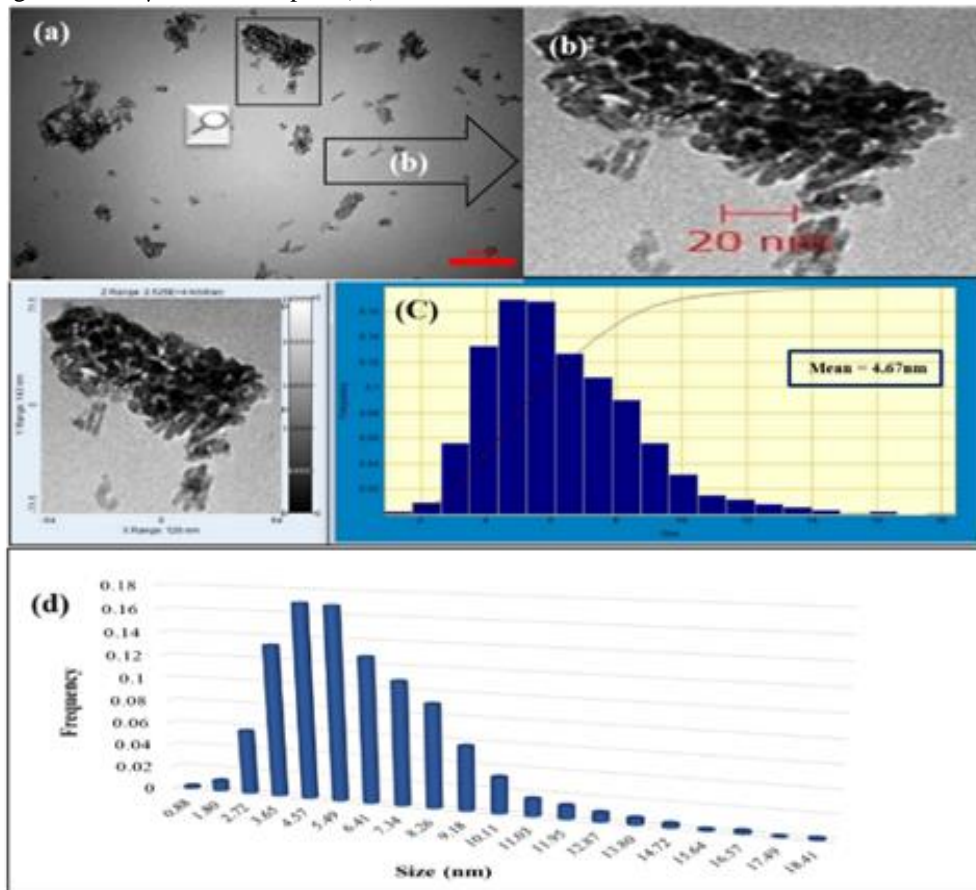
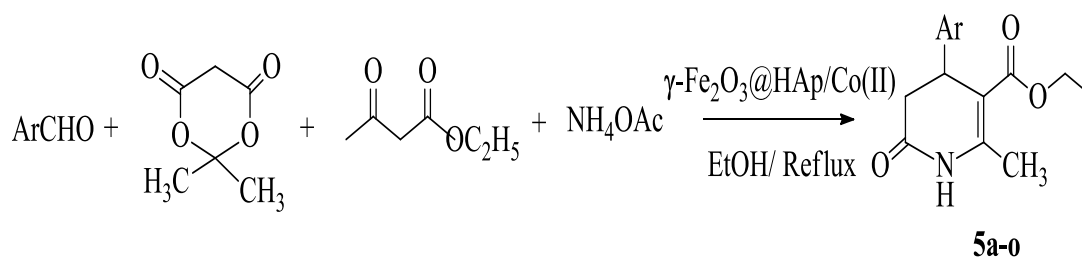


Fig.7. (a, b) TEM micrographs of  $\gamma\text{-Fe}_2\text{O}_3\text{@HAp/Co(II)}$  (c, d)  $\gamma\text{-Fe}_2\text{O}_3\text{@HAp/Co(II)}$  nanoparticle size distribution diagram



Ar = C<sub>6</sub>H<sub>5</sub>, 3-O<sub>2</sub>NC<sub>6</sub>H<sub>4</sub>, 2-O<sub>2</sub>NC<sub>6</sub>H<sub>4</sub>, 2-ClC<sub>6</sub>H<sub>4</sub>, 4-ClC<sub>6</sub>H<sub>4</sub>, 3-ClC<sub>6</sub>H<sub>4</sub>, 2,4-Cl<sub>2</sub>C<sub>6</sub>H<sub>3</sub>, 3-MeOC<sub>6</sub>H<sub>4</sub>, 2-MeOC<sub>6</sub>H<sub>4</sub>, 2,6-Cl<sub>2</sub>C<sub>6</sub>H<sub>3</sub>, 4-MeC<sub>6</sub>H<sub>4</sub>, 3-MeC<sub>6</sub>H<sub>4</sub>, 2-BrC<sub>6</sub>H<sub>4</sub>, 4-BrC<sub>6</sub>H<sub>4</sub>, 3-MeO-4-HOC<sub>6</sub>H<sub>3</sub>

**Scheme 2.** Synthesis of 3,4-dihydropyridones derivatives using  $\gamma$ -Fe<sub>2</sub>O<sub>3</sub>@HAp/Co(II).

**Table 1.** Optimization of the reaction conditions<sup>a</sup>

Entry	Solvent	Catalyst	Temp (°C)	Time	Yield (%) <sup>b</sup>
1	H <sub>2</sub> O	$\gamma$ -Fe <sub>2</sub> O <sub>3</sub> @HAp/Co(II)	100	360	80
2	DMF	$\gamma$ -Fe <sub>2</sub> O <sub>3</sub> @HAp/Co(II)	120	120	70
3	Toluene	$\gamma$ -Fe <sub>2</sub> O <sub>3</sub> @HAp/Co(II)	110	160	60
4	THF	$\gamma$ -Fe <sub>2</sub> O <sub>3</sub> @HAp/Co(II)	65	200	35
5	EtOH/H <sub>2</sub> O	$\gamma$ -Fe <sub>2</sub> O <sub>3</sub> @HAp/Co(II)	80	180	64
6	EtOH	$\gamma$ -Fe <sub>2</sub> O <sub>3</sub> @HAp/Co(II)	78	25	95
7	EtOH	$\gamma$ -Fe <sub>2</sub> O <sub>3</sub> @HAp/Co(II)	60	90	71
8	EtOH	$\gamma$ -Fe <sub>2</sub> O <sub>3</sub> @HAp/Co(II)	70	60	89
10	EtOH	$\gamma$ -Fe <sub>2</sub> O <sub>3</sub> @HAp/Co(II)	r.t.	185	trace
11	EtOH	$\gamma$ -Fe <sub>2</sub> O <sub>3</sub> @HAp/Pd(II)[29]	78	60	90
12	EtOH	<i>p</i> -TSA	78	240	75
13	EtOH	AcOH	78	180	80
14	EtOH	NEt <sub>3</sub>	78	720	57
15	EtOH	DBU	78	720	50
16	EtOH	DABCO	78	720	60
17	EtOH	-	78	144	30

<sup>a</sup>Reaction conditions: meldrum's acid (1.0 mmol), ethyl acetoacetate (1.0 mmol), 4-bromobenzaldehyde (1.0 mmol), ammonium acetate (3.0 mmol), catalyst (0.22 mol%), solvent (2 mL).

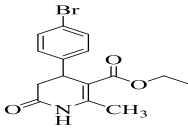
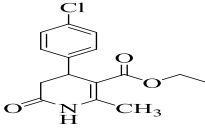
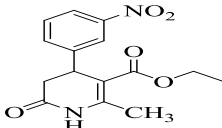
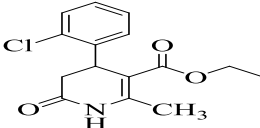
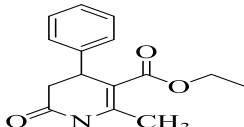
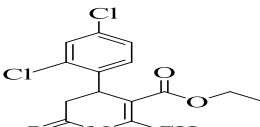
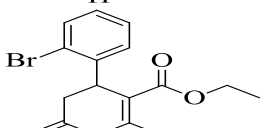
<sup>b</sup>Isolated yields

**Table 2.** Optimization of the amount of  $\gamma\text{-Fe}_2\text{O}_3\text{@HAp/Co(II)}$  in the model reaction<sup>a</sup>.

Entry	$\gamma\text{-Fe}_2\text{O}_3\text{@HAp/Co(II)}$ (mg)	Time(min)	Yield <sup>b</sup> (%) <sup>b</sup>
1	10	25	95
2	5	60	65
3	20	25	95
4	-	1440	30

<sup>a</sup>Reaction conditions: Meldrum's acid (1.0 mmol), ethyl acetoacetate (1.0 mmol), 4-bromobenzaldehyde (1.0 mmol), ammonium acetate (3.0 mmol),  $\gamma\text{-Fe}_2\text{O}_3\text{@HAp/Co(II)}$  (10 mg, 0.22 mol%), ethanol (2 mL), 78°C, 25 min. <sup>b</sup>Isolated yield.

**Table 3.** Synthesis of 3,4-dihydropyridone derivatives (5a-o) in the presence of novel  $\gamma\text{-Fe}_2\text{O}_3\text{@HAp/Co(II)}$  under optimized reaction conditions<sup>a</sup>.

Entry	product	Structure	Time(min)	Yield(%) <sup>b</sup>	M.P. (°C)	
					Observed	Reported
1	5a		25	95	185-187	-
2	5b		20	90	176-178	178-179 [32]
3	5c		45	78	166-169	168-170 [32]
4	5d		35	90	180-182	182-181 [32]
5	5e		30	85	168-170	170-168 [32]
6	5f		20	92	180-183	-
7	5g		30	82	189-192	-

8	5h		50	70	200-202	201-202 [32]
9	5i		75	71	161-164	-
10	5j		60	70	185-187	-
11	5k		35	80	182-184	-
12	5l		20	92	233-235	-
13	5m		45	70	291-294	-
14	5n		35	80	131-133	-
15	5o		25	90	177-180	-

<sup>a</sup>Reaction conditions: Meldrum's acid (1.0 mmol), ethyl acetoacetate (1.0 mmol), aromatic aldehyde (1.0 mmol), ammonium acetate (3.0 mmol),  $\gamma$ -Fe<sub>2</sub>O<sub>3</sub>@HAp/Co(II) (10 mg, 0.22 mol%), ethanol (2 mL), 78 °C.

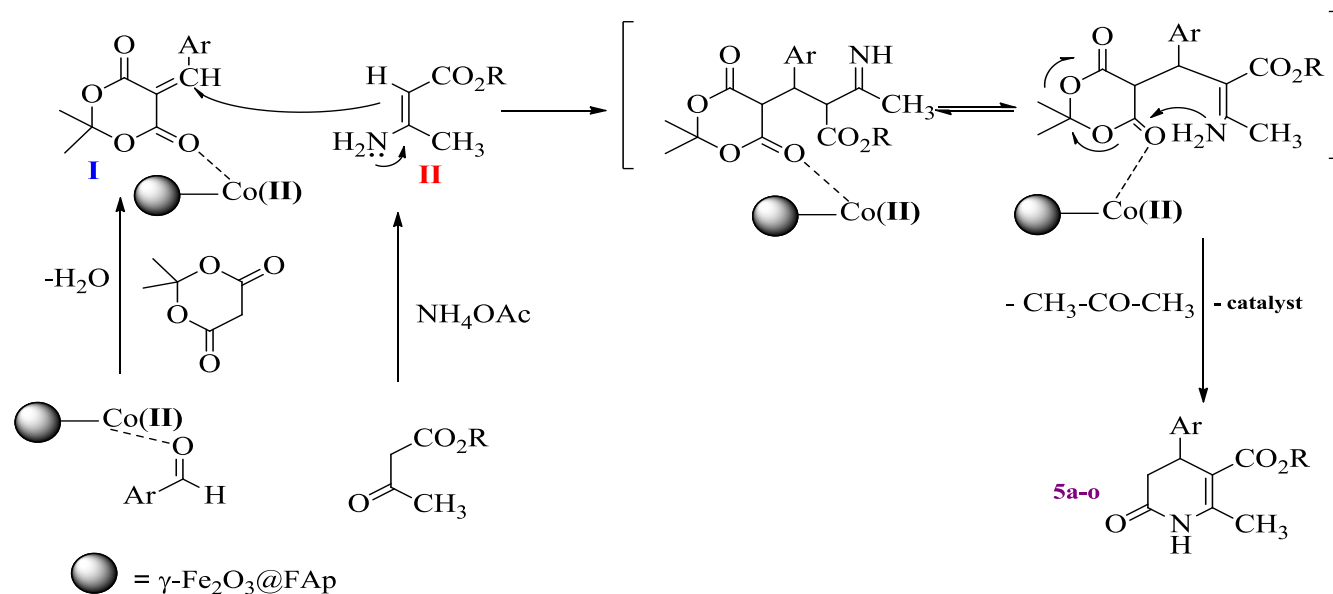
<sup>b</sup>Isolated yields.

**Table 4.** Comparison of  $\gamma$ -Fe<sub>2</sub>O<sub>3</sub>@HAp/Co(II) and various catalysts in the synthesis of 3,4-dihydropyridone.

Entry	Catalyst	Solvent	Condition	Time (min)	Yield <sup>a</sup> (%) <sup>a</sup>
1	$\gamma$ -Fe <sub>2</sub> O <sub>3</sub> @HAp/Pd(II)	EtOH	Reflux (78 °C)	60	90 [29]
2	$\gamma$ -Fe <sub>2</sub> O <sub>3</sub> @HAp/Co(II)	EtOH	Reflux (78 °C)	25	95 (This work)
3	SBA-Pr-SO <sub>3</sub> H	-	Heating (140 °C)	40	90 [21]
4	SiO <sub>2</sub> -Pr-SO <sub>3</sub> H	-	Heating (140 °C)	32	93 [22]
5	AcOH	-	Reflux (119 °C)	600	65 [32]

<sup>a</sup> Yield of isolated product.

A plausible mechanism for the synthesis of 3,4-dihydropyridone derivatives is presented in (Scheme 3). The reaction proceeds through several successive steps [32]. A Hantzsch-like mechanism operates in the synthesis of target products. The intermediate I, resulted from the Knoevenagel reaction of Meldrum's acid and corresponding aryl aldehyde, reacts with enamine II formed by the reaction of  $\beta$ -ketoester and ammonia. A Michael-type addition of enamine II on ylidene I followed by an intramolecular cyclization reaction gives rise to the desired products **5a-o**.



**Scheme 3.** A proposed mechanism for the synthesis of 3,4-dihydropyridones in the presence of  $\gamma\text{-Fe}_2\text{O}_3\text{@HAp/Co(II)}$ .

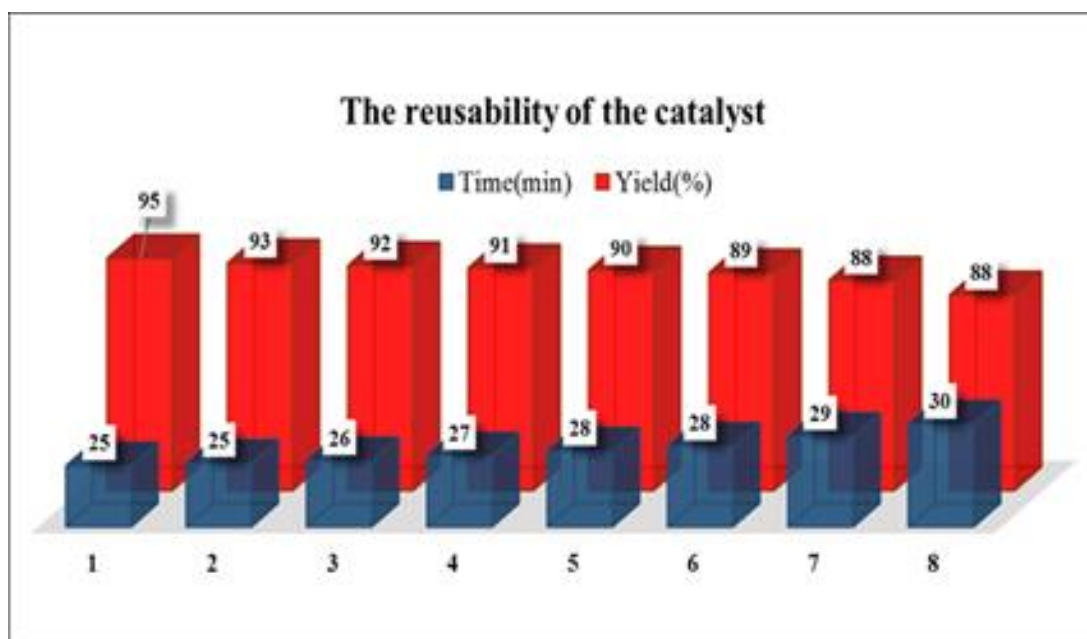


**Fig. 8.** Reusability of  $\gamma\text{-Fe}_2\text{O}_3\text{@HAp/Co(II)}$  in the synthesis of 3,4-dihydropyridone **5a** under optimized reaction conditions.

#### 4. Conclusions

A new and highly effectual HAp-encapsulated- $\gamma$ -Fe<sub>2</sub>O<sub>3</sub>-based Co(II) organic-inorganic hybrid nanocatalyst ( $\gamma$ -Fe<sub>2</sub>O<sub>3</sub>@HAp/Co(II)) was successfully introduced for the green and impressive synthesis of a diverse series of 3,4-dihydropyridones. This method has several impactful benefits, such as benign conditions, higher yields, lower reaction times, straightforward work-up procedure, easy recovery of the catalyst, use of sustainable catalyst, and ethanol as a green solvent. The recovered catalyst can be reused in eight consecutive runs without a significant decline in its catalytic efficiency.

#### Acknowledgements

The authors gratefully acknowledge the technical support provided by Islamic Azad University of Rasht Branch.

#### References

- [1] E. Ruijter, R. Scheffelaar, R. V. A. Orru, *Angew* 50 (2011) 6234-6246.
- [2] I. V. Magedov, A. Kornienko, *Chem. Heterocycl. Compd.* 48 (2012) 33-38.
- [3] R. Dua, S. Shrivastava, S. K. Sonwane, S. K. Srivastava, *Adv. Biol. Res.* 5 (2011) 120-144.
- [4] H. S. Hilal, M. S. Ali-Shtayeh, R. Arafat, T. Al-Tel, W. Voelter, A. Barakat, *Eur. J. Med. Chem.* 41 (2006) 1017-1024.
- [5] R. Budriesi, A. Bisi, P. Ioan, A. Rampa, S. Gobbi, F. Belluti, L. Piazzini, P. Valenti, A. Chiarini, *Bioorg. Med. Chem.* 13(2005), 3423-3430.
- [6] L. Navidpour, H. Shafaroodi, R. Miri, A. R. Dehpour, A. Shafiee, *Farmaco* 59 (2004) 261-269.
- [7] I. Adachi, T. Yamamori, Y. Hiramatsu, K. Sakai, S-I. Mihara, M. Kawakami, M. Masui, O. Uno, M. Ueda, *Chem. Pharm. Bull.* 36 (1988) 4389-4402.
- [8] R. Preston Mason, *Cerebrovasc. Dis.* 16 (2003) 11-17.
- [9] S. Yamagishi, T. Matsui, K. Nakamura, *Med. Hypotheses* 68 (2007) 1096-1098.
- [10] G. Duburs, B. Vigante, A. Plotniece, A. Krauze, A. Sobolevs, J. Briede, V. Kluša, A. Velena, *Med. Chem.* 26(2008) 68-70.
- [11] A. Hantzsch, *Jus. Lie. Ann. Chim.* 215 (1882) 1-82.
- [12] N. C. Desai, A. M. Dodiya, N. R. Shihory, *Med. Chem. Res.* 21 (2012) 2579-2586.
- [13] M. Nuchter, B. Ondruschka, A. Jungnickel, U. Muller, *J. Phys. Org. Chem.* 13(2000) 579-586.
- [14] H. Rodriguez, O. Reyes, M. Suarez, H. Garay, R. Perez, J. Cruz, Y. Verdecia, N. Martin, C. Seoane, *Tetrahedron lett.* 43 (2002) 439-441.
- [15] H. Rodriguez, M. Suarez, R. Perez, A. Petit, A. Loupy, *Tetrahedron lett.* 44 (2003) 3709-3712.
- [16] G. Mohammadi Ziarani, S. Mousavi, N. Lashgari, A. Badiei, *J. Chem. Sci.* 125 (2013) 1359-1364.
- [17] A. Modarres Hakimi, N. Lashgari, S. Mahernia, G. Mohammadi Ziarani, M. Amanlou, *Res Pharm Sci.* 12 (2017) 353-363
- [18] N. A. Hamdy, A. M. Gamal-Eldeen, *Eur. J. Med. Chem.* 44(2009) 4547-4556.
- [19] G. Mohammadi Ziarani, A. R. Badiei, Y. Khaniania, M. Haddadpour, *Iran. J. Chem. Chem. Eng.* 29 (2010) 1-10.
- [20] G. Mohammadi Ziarani, A. Badiei, F. Shahjafari, T. Pourjafar, *S. Afr. J. Chem.* 65 (2012) 10-13.
- [21] G. Mohammadi Ziarani, A. Abbasi, A. Badiei, Z. Aslani, *Eur. J. Chem.* 8(2011)293-299.
- [22] N. Lashgari, G. Mohammadi Ziarani, A. Badiei, P. Gholamzadeh, *Eur. J. Chem.* 3 (2012) 310-313.
- [23] L. Ma'mani, M. Sheykhani, A. Heydari, M. Faraji, Y. Yamini, *Appl. Catal. A-Gen.* 377 (2010) 64-69.
- [24] M. Khoobi, L. Ma'mani, F. Rezazadeh, Z. Zareie, A. Foroumadi, A. Ramazani, A. Shafiee, *J. Mol. Catal. A* 359 (2012) 74-80.
- [25] M. Sheykhani, M. Mohammadquli, A. Heydari, *J. Mol. Struct.* 1027 (2012) 156-161.
- [26] M. Mohsenimehr, M. Mamaghani, F. Shirini, M. Sheykhani, F. Azimian Moghaddam, *Chinese Chem. Lett.* 25 (2014) 1387-1391.
- [27] L. Ma'mani, M. Sheykhani, A. Heydari, *Appl. Catal. A-Gen.* 395 (2011) 34-38.
- [28] M. Sheykhani, L. Ma'mani, A. Ebrahimi, A. Heydari, *J. Mol. Catal. A-Chem.* 335 (2011) 253-261.
- [29] M. Barazandehdoust, M. Mamaghani, H. Kefayati, *React. Kinet. Mech. Cat.* 129 (2020) 1007-1026.
- [30] Bd. Cullity, *Elements of X-ray diffraction*. Third Edition Addison-Wesley Publishing Company, London (1956).
- [31] S. Thomas, K. Joseph, S. K. Malhotra, K. Goda, M. S. Sreekala, *Polymer composites, nanocomposites*. Wiley-VCH Weinheim 2 (2013).
- [32] E. Ruiz, H. Rodríguez, J. Coro, E. Salfrán, M. Suárez, R. Martínez-Alvarez, N. Martín, *Ultrason. Sonochem.* 18 (2011) 32-36.